Performance evaluation of thermoelectric device for thermal vacuum testing of nanosatellites

Joseph Ampadu OFOSU, Hirokazu MASUI, and Mengu CHO

Center for Nanosatellite Testing, Kyushu Institute of Technology, Kitakyushu, Japan
Laboratory of Lean Satellite Enterprises and In-Orbit Experiments, Kyushu Institute of Technology, Kitakyushu, Japan

(Received January 11th, 2022)

Nano and micro satellites are progressively becoming the backbone or platform via which academia, industry and governments across the globe pursue space for research and education, economics, technological demonstration, security and many more. This concept is making space accessible, affordable, and reliable, especially for new entrants in the space field. One of the ways to achieve this is making environmental testing of satellites inexpensive. We present in this paper, the performance evaluation of a comparatively inexpensive thermal vacuum testing system, equipped with a thermoelectric device that uses the Peltier principle of heat generation and/ or absorption. The thermoelectric device is a commercial-off-the-shelf (COTS) component with a cooling capacity of 16.9 W. The testing system does not require liquified nitrogen or silicon oil for simulating cold conditions. In addition, the testing system is capable of vacuum thermal cycling and balancing tests within -45 ℃ to +75 ℃, well beyond the minimum requirements of the ISO-19683. These characteristics make the testing system simple, reproducible, and affordable. We evaluated performance parameters of the Peltier device as functions of cold side temperature.

Key Words: Figure of merit, Thermal vacuum testing, Thermoelectric device, CubeSat

Nomenclature

I	:	current, A
k	:	thermal conductance, W/K
Q	:	thermal power, W
R	:	resistance, Ω
S	:	Seebeck coefficient, V/K
T	:	temperature, K
V	:	voltage, V
ZT	:	device figure of merit
Δ	:	change/ difference
π	:	Peltier coefficient, V
Subscripts		
c	:	cold side
h	:	hot side
j	:	dissipated
p	:	Peltier element/ device

1. Introduction

Thermal vacuum testing (TVT) is a key component of environmental testing, required for CubeSat system qualification and/ or acceptance. We have endeavored to carry out TVT using a thermoelectric device. Thermoelectric modules (TEMs) are solid-state devices that use thermoelectric effects for energy conversion between thermal and electrical forms. The energy conversion process is defined by Seebeck, Peltier and Thomson effects, together with the principles of Joule heating and Fourier conduction.[1)] Advances in semiconductor technology,[2–4)] the possible applications and the attractive features of TEMs have focused lots of research efforts on thermoelectric devices. Some features of TEMs include compact in size, no moveable parts hence simple and maintenance-free, no requirements for refrigerants, have high energy density, adaptable and environmentally clean.[2,5–7)] TEMs are grouped as thermoelectric coolers (TECs) which are used for cooling/ heating applications and thermoelectric generators (TEGs) for electricity generation from temperature gradients.[8–10)] TEC applications include thermal management of optical devices such as lasers, intensified charge coupled devices, and processing units of computational devices. TEG applications include electricity generation in space missions, thermocouple sensors, and possibly, waste heat harvesting from the exhaust of automobiles.[11–15)] One disadvantage of TEMs especially TEG devices is their low energy conversion efficiency which limits applications to low power systems and thus economically unbeneficial compared with conventional energy generators.[16,17)] Nonetheless, numerous research efforts via analytical,[18–21)] numerical simulation[22–25)] and experimental studies[26–30)] are being carried out to improve the thermoelectric conversion efficiency of TEMs.

The number of small satellites launches have been on the rise in recent years, and as indicated by BryceTech, the year 2020 received 40% of all smallsats launched in the past 10 years. Of the 1202 smallsats launched in 2020, 11% and 3% were respectively for remote sensing and technology development.[31)] Most of these were of the Nano and Micro satellite categories. With Kyushu Institute of Technology as the academic institute with the highest number of satellites launched in the past 10 years, the Center for Nanosatellite Testing (CeNT) is working toward the objective of making space accessible, inexpensive, and reliable for new entrants in the space field.

In this study, we present the progress of ongoing work on an

inexpensive thermal vacuum testing (TVT) system at CeNT. This TVT system which has been used in testing an engineering model of a 1U CubeSat does not require the supply of liquid nitrogen (LN_2) for cooling and has been extensively described in reference 32). The TVT system uses a pair of TEMs for both cooling and heating based on the Peltier effect principle. In the following sections, we present the thermal unit of the TVT,[33] no-load and load conditions tests, as well as the evaluation of the thermoelectric device figure of merit, ZT.

2. 2. The thermal unit[33]

The thermal unit shown in Fig. 1 comprises two 4-stage Peltier element sandwiched between a copper (Cu) shroud plate and an aluminum (Al) heat sink. A compressible thermal gap filler for minimizing contact thermal resistance is interfaced between the elements at the top with the Cu plate and at the bottom with the Al heatsink. The heatsink is equipped with Cu piping for effective heat dissipation. The entire unit is isolated from the chamber wall using 4 PTFE support bases as shown in Fig. 2.

The shroud part of the thermal unit which holds test articles, is made up of the Cu plate and a Cu sheet; thermally insulated from each other by a room-temperature-vulcanizing (RTV) adhesive. The interior of the shroud is black coated to increase radiative emissivity and absorptivity. The entire shroud is covered with a multi-layer insulation (MLI) material to minimize heat losses as the chamber is always at room temperature conditions. PTFE spacers are used to support the weight of the Cu shroud and serve as thermal isolators between the Cu shroud and the Al heatsink. Heat dissipation from the Al heatsink is achieved by circulating coolant/fluid at a maximum flow rate of 20 liters/ minute. Table 1 shows the physical,

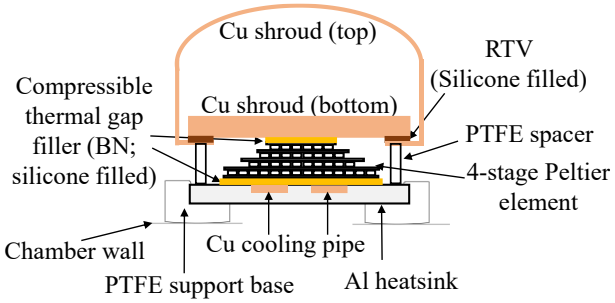

Fig. 1. Schematic representation of the thermal unit.

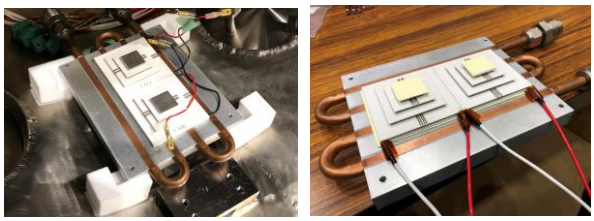

Fig. 2. Pictures of the Peltier elements, Al heatsink, PTFE blocks and thermal gap filler.

Table 1. Thermal unit components' properties.

4-stage Peltier element	
Manufacturer	Kryotherm
Module name	TB-4-(199-97-49-17)-1.5
Maximum current, A	6.7
Maximum voltage, V	23.6
Max temp. difference, ℃ (or K)	111
AC resistance, Ω	3.42
Operating temperature, ℃	-50 - +80
Thermal gap filler	
Manufacturer	Laird Technologies
Model number	TPLI 240
Composition	Boron nitride with silicone
Thickness, mm	1.02
Density, g/ cc	1.43
Outgassing CVCM, %	0.02
Operating temperature, ℃	-45 - +200
Thermal conductivity, (W/ mK)	6
AC Breakdown voltage, V	> 5000
Room-temperature-vulcanizing adhesive	
Manufacturer	Wacker-Chemie GmbH
Model number	RTV S 691
Specific gravity	1.41 – 1.43
Thermal conductivity, (W/ m℃)	0.39
Operating temperature, ℃	-180 - +200
Circulator and coolant	
Manufacture, Model	Axel, LTC1200a
Circulator capacity, L	16
Max. flow rate, L/ min	20
Operating temperature, ℃	-20 - +30
Coolant	Ethylene glycol (90-94 wt%)
Coolant: deionized water mix. ratio	0.4:0.6

thermal, and electrical properties of some components of the thermal unit.

3. Vacuum test runs[33]

In this section, we present thermal vacuum test runs for both no-load condition and a 1U CubeSat, using the configuration of Fig. 1. The 1U satellite was an engineering model (EM), courtesy the 5th generation the Joint Global Multi-Nations Birds Satellite (BIRDS 5) project. The TEM/ Peltier elements were operated at approximately 33% of their current and voltage ratings; respectively 2 A and 8 V. In order to achieve a minimum coolant temperature of -25 ℃, the mixture ratio of coolant to deionized water was set as 0.4:0.6.

3.1. No-load test

Figure 3 shows the temperature and pressure profiles of the no-load test conducted for about 32 hours. Two cycles were performed with a dwell time in the first cycle at approximately 2 hours. This is typical for vacuum thermal cycling tests of CubeSats. The dwell time for the second cycle was about 8 hours, which is also typical for the vacuum thermal balance tests of satellites. To achieve heating, the polarity of the Peltier elements was reversed at the same current voltage levels.

As shown in Fig. 3, the worst cold and hot case temperatures were -45 ℃ and +75 ℃ respectively for the Cu shroud plate, well beyond the minimum requirements of the ISO-19683 standard. The temperature difference between the shroud bottom and the shroud top was about 5 ℃ during the entire test. This shows that radiative heating/ cooling was efficient because, both the shroud bottom and top were thermally isolated. During cooling, the top part of Peltier element transfers heat to the bottom whiles the reverse action occurs when heating. To avoid exceeding the maximum temperature difference between the hot and cold side plates of the Peltier element (i.e. 111 K), the coolant temperature was set to -15 ℃ and +25 ℃ during cooling and heating respectively.

3.2. BIRDS 5 EM testing

Figures 4 and 5 show the BIRDS 5 1U EM satellite overview and the placement of thermocouple sensors on some subsystem components. The temperature and pressure profiles of the test are shown in Fig. 6 for a continuous test period of 65 hours. First, a cycle of cooling and heating was performed, followed by a room temperature soak, and ending with another cycle of cooling and heating. The attained worst cold and hot case temperatures were -8 ℃ and +55 ℃ respectively, defined by the battery operating

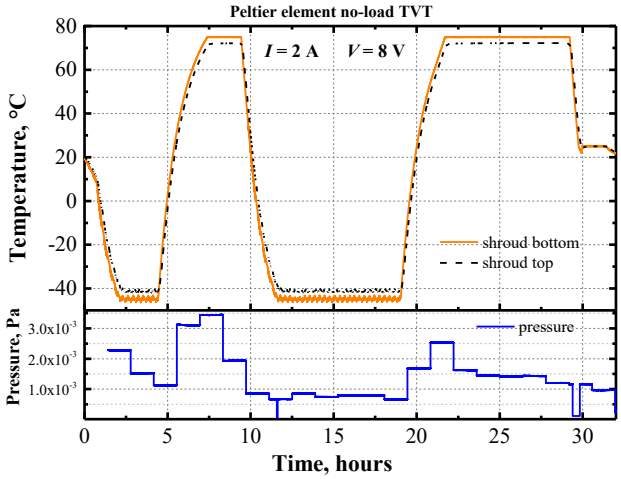

Fig. 3. Temperature and pressure profiles at no-load conditions.

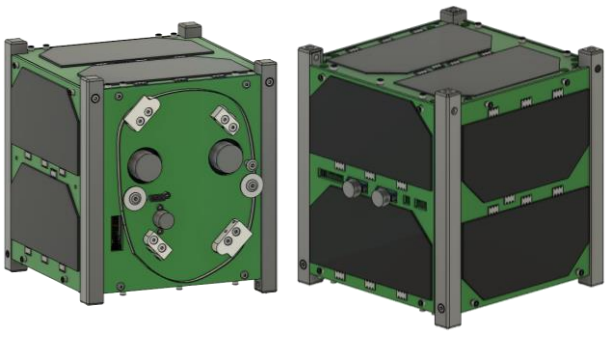

Fig. 4. BIRDS 5 configuration/ overview.

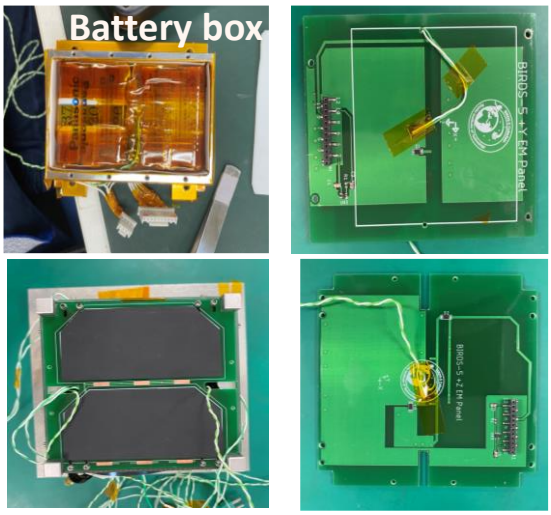

Fig. 5. Placement of thermocouple sensors on battery box and external panels.

temperature range. The ramp rate for the entire test was approximately ±0.4 ℃/ min. For a perspective, the ramp rate was quite similar to those of our regular chambers (±0.5 ℃/ min) at CeNT. However, the ramp rate for heating was about half that of our heaters used in our regular chambers.

Comparatively, a typical 2-cycle TVT test of a 1U CubeSat at CeNT, requires about 2 kPa usage of LN_2 supply. This is costed as 20,400 JPY (2 kPa × 136 kg/ kPa × 75 JPY/ kg) and is equivalent to a unit cost of the 4-stage TEM (US$ 225) used in this study. More so, a typical test would require at least 4 DC power supplies compared to the 1 and/ or 2 used in this study. Thus, the running cost comparison evidently shows that, the TEM device is a cost-effective option compared to the conventional way of testing, without even considering the equipment cost for LN_2.

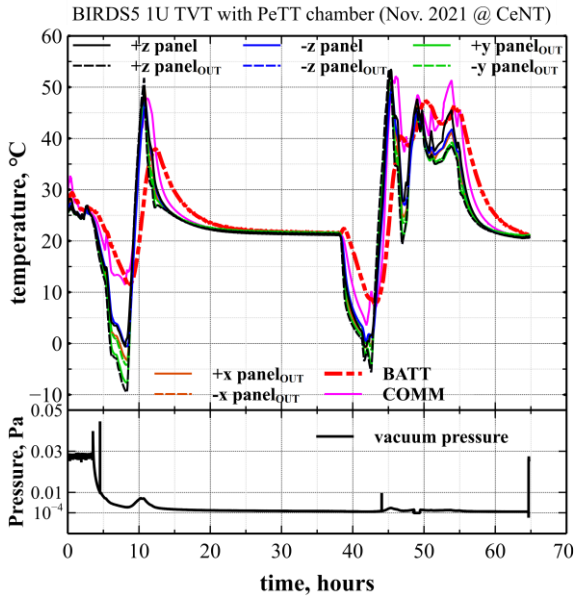

Fig. 6. Temperature and pressure profiles of BIRDS 5 EM test.

4. Performance parameters

TEM resistance R_p, Seebeck coefficient S, thermal conductance k and the device figure of merit ZT were evaluated using measured temperature, with drawn voltage and current quantities during the thermal vacuum test. Considering the simplified thermal power flow schematic for a TEM shown in Fig. 7, as well as the following assumptions:

1. A uniform 1-dimensional heat flow with non-ideal heat and electrical losses
2. Exactly matched n- and p-type couples, where cooling/ heating are concentrated at interfaces, then

The following equations and expressions can be derived:

$$R_p = \left(\frac{V_p}{I_p}\right)\left(\frac{T_c}{T_h}\right) \quad (1)$$

$$S = \left(\frac{V_p}{T_h}\right) \quad (2)$$

$$k \propto SI_p\frac{T_c}{\Delta T} \quad (3)$$

$$ZT = \frac{S^2}{R_p k}T, \quad T = \frac{T_c + T_h}{2} \quad (4)$$

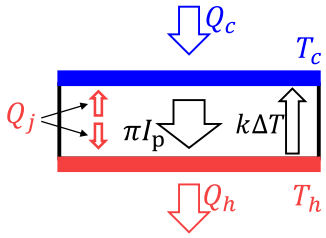

Fig. 7. Schematic of thermal power distribution in a TEM.

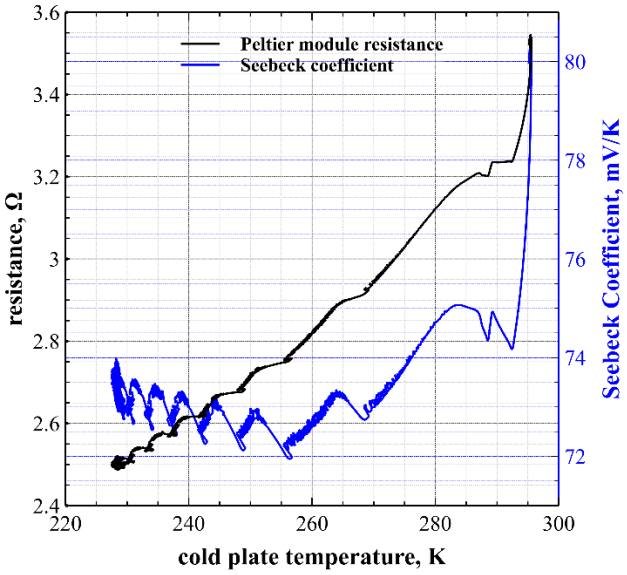

Fig. 8. Plots of R_p and S as functions of T_c.

Figure 8 shows the plots of R_p and S as functions of T_c. Both parameters decreased with cooling as expected. R_p at room temperature (and vacuum condition) was equivalent to the AC resistance (3.4 Ω) as specified by the manufacturer.

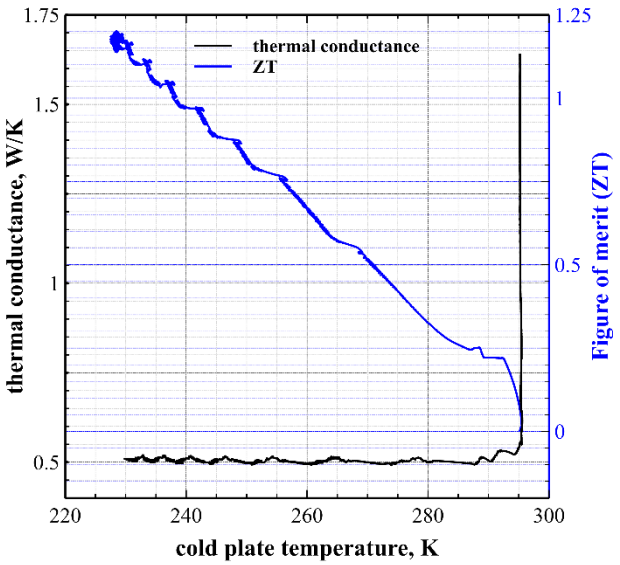

Fig. 9. Plots of k and ZT as functions of T_c.

In Fig. 9, ZT increased with cooling whiles k remained independent of T_c due to the assumptions made. The high value of k at high T_c is unusual and due to ZT approaching zero at room temperature condition.

5. Summary

We have demonstrated the applicability of a thermoelectric device based on the principle of Peltier effect to thermal vacuum testing of a 1U CubeSat. Using two 4-stage Peltier devices, and running them at 33% of their electrical ratings, temperatures within -45 ℃ to +75 ℃ were attained, well beyond the minimum requirements of the ISO-19683. These make the testing system simple, accessible, and affordable. Performance parameters such as device figure of merit ZT and Seebeck coefficient S were evaluated as functions of T_c. We intend to improve the system performance of the TEM-based thermal vacuum testing system and hope that it would facilitate the growth of scientific, and technical endeavors within the CubeSat community.

Acknowledgments

The authors would like to thank members of the BIRDS 5 project for permitting the use of their 1 U EM satellite in this study. We also appreciate the efforts of the project members who assisted with the testing.

References

1) Goldsmid, H. J.: The Thermoelectric and Related Effects, *Springer Ser. Mater. Sci.*, **121** (Springer, Berlin, Heidelberg, 2010), pp. 1–6.
2) *Thermoelectrics Handbook*, Thermoelectrics Handbook (2018) doi:10.1201/9781420038903.

3) Goldsmid, H. J. and Douglas, R. W.: The Use of Semiconductors in Thermoelectric Refrigeration, *Br. J. Appl. Phys.*, **5** (IOP Publishing, 1954), pp. 386–390.
4) Hicks, L. D. and Dresselhaus, M. S.: Thermoelectric Figure of Merit of a One-Dimensional Conductor, *Phys. Rev. B*, **47** (1993), pp. 16631–16634.
5) Zebarjadi, M., Esfarjani, K., Dresselhaus, M. S., Ren, Z. F. and Chen, G.: Perspectives on Thermoelectrics: From Fundamentals to Device Applications, *Energy Environ. Sci.*, **5** (Royal Society of Chemistry, 2012), pp. 5147–5162.
6) Disalvo, F. J.: Thermoelectric Cooling and Power Generation, *Science (80-.).*, **285** (Switzer-land, 1999), pp. 703–706.
7) Riffat, S. B. and Ma, X.: Thermoelectrics: A Review of Present and Potential Applications, *Appl. Therm. Eng.*, **23** (Pergamon, 2003), pp. 913–935.
8) Ioffe, A. F., Stil'bans, L. S., Iordanishvili, E. K., Stavitskaya, T. S., Gelbtuch, A. and Vineyard, G.: Semiconductor Thermoelements and Thermoelectric Cooling, *Phys. Today*, **12** (American Institute of PhysicsAIP, 1959), pp. 42.
9) Wen, S., Zhang, G., Dan, Y., Wang, D. and Deng, M.: Model Output Following Control for an Aluminum Plate Cooling Process with a Peltier Device, The 2012 International Conference on Advanced Mechatronic Systems (2012).
10) Wang, C. C., Hung, C. I. and Chen, W. H.: Design of Heat Sink for Improving the Performance of Thermoelectric Generator Using Two-Stage Optimization, *Energy*, **39** (Pergamon, 2012), pp. 236–245.
11) Basti, A., Obikawa, T. and Shinozuka, J.: Tools with Built-in Thin Film Thermocouple Sensors for Monitoring Cutting Temperature, *Int. J. Mach. Tools Manuf.*, **47** (Pergamon, 2007), pp. 793–798.
12) El-Genk, M. S., Saber, H. H. and Caillat, T.: Efficient Segmented Thermoelectric Unicouples for Space Power Applications, *Energy Convers. Manag.*, **44** (Pergamon, 2003), pp. 1755–1772.
13) Samson, D., Kluge, M., Fuss, T., Schmid, U. and Becker, T.: Flight Test Results of a Thermoelectric Energy Harvester for Aircraft, *J. Electron. Mater. 2012 416*, **41** (Springer, 2012), pp. 1134–1137.
14) Longtin, J. P. *et al.*: Fabrication of Thermoelectric Devices Using Thermal Spray: Application to Vehicle Exhaust Systems, *J. Therm. Spray Technol. 2013 225*, **22** (Springer, 2013), pp. 577–587.
15) Lu, C., Wang, S., Chen, C. and Li, Y.: Effects of Heat Enhancement for Exhaust Heat Exchanger on the Performance of Thermoelectric Generator, *Appl. Therm. Eng.*, **89** (Pergamon, 2015), pp. 270–279.
16) Harman, T. C., Walsh, M. P., laforge, B. E. and Turner, G. W.: Nanostructured Thermoelectric Materials, *J. Electron. Mater. 2005 345*, **34** (Springer, 2005), pp. L19–L22.
17) Vining, C. B.: An Inconvenient Truth about Thermoelectrics, *Nat. Mater. 2009 82*, **8** (Nature Publishing Group, 2009), pp. 83–85.
18) Lineykin, S. and Ben-Yaakov, S.: Modeling and Analysis of Thermoelectric Modules, *IEEE Trans. Ind. Appl.*, **43** (2007), pp. 505–512.
19) Wu, Y., Zuo, L., Chen, J. and Klein, J. A.: A Model to Analyze the Device Level Performance of Thermoelectric Generator, *Energy*, **115** (Elsevier Ltd, 2016), pp. 591–603.
20) Bjørk, R., Christensen, D. V., Eriksen, D. and Pryds, N.: Analysis of the Internal Heat Losses in a Thermoelectric Generator, *Int. J. Therm. Sci.*, **85** (Elsevier Masson SAS, 2014), pp. 12–20.
21) Shen, R., Gou, X., Xu, H. and Qiu, K.: Dynamic Performance Analysis of a Cascaded Thermoelectric Generator, *Appl. Energy*, **203** (Elsevier Ltd, 2017), pp. 808–815.
22) Fang, E., Wu, X., Yu, Y. and Xiu, J.: Numerical Modeling of the Thermoelectric Cooler with a Complementary Equation for Heat Circulation in Air Gaps, *Open Phys.*, **15** (2017), pp. 27–34.
23) Manikandan, S. and Kaushik, S. C.: The Influence of Thomson Effect in the Performance Optimization of a Two Stage Thermoelectric Generator, *Energy*, **100** (Elsevier Ltd, 2016), pp. 227–237.
24) Meng, F., Chen, L. and Sun, F.: A Numerical Model and Comparative Investigation of a Thermoelectric Generator with Multi-Irreversibilities, *Energy*, **36** (Elsevier Ltd, 2011), pp. 3513–3522.
25) Högblom, O. and Andersson, R.: A Simulation Framework for Prediction of Thermoelectric Generator System Performance, *Appl. Energy*, **180** (2016), pp. 472–482.
26) Wang, S., Xie, T. and Xie, H.: Experimental Study of the Effects of the Thermal Contact Resistance on the Performance of Thermoelectric Generator, *Appl. Therm. Eng.*, **130** (Elsevier Ltd, 2018), pp. 847–853.
27) Bjørk, R., Sarhadi, A., Pryds, N., Lindeburg, N. and Viereck, P.: A Thermoelectric Power Generating Heat Exchanger: Part i - Experimental Realization, *Energy Convers. Manag.*, **119** (2016), pp. 473–480.
28) Liang, X., Sun, X., Tian, H., Shu, G., Wang, Y. and Wang, X.: Comparison and Parameter Optimization of a Two-Stage Thermoelectric Generator Using High Temperature Exhaust of Internal Combustion Engine, *Appl. Energy*, **130** (Elsevier Ltd, 2014), pp. 190–199.
29) Amaral, C., Brandão, C., Sempels, É. V. and Lesage, F. J.: Net Thermoelectric Generator Power Output Using Inner Channel Geometries with Alternating Flow Impeding Panels, *Appl. Therm. Eng.*, **65** (Elsevier Ltd, 2014), pp. 94–101.
30) Hsu, C. T., Huang, G. Y., Chu, H. S., Yu, B. and Yao, D. J.: Experiments and Simulations on Low-Temperature Waste Heat Harvesting System by Thermoelectric Power Generators, *Appl. Energy*, **88** (Elsevier Ltd, 2011), pp. 1291–1297.
31) BryceTech: Smallsats by the Numbers, (2021).
32) Bonsu, B., Masui, H. and Cho, M.: Peltier-Based Thermal Testing (PeTT) Vacuum Chamber: Affordable Testing Facility for Lean Satellites, *UNISEC Sp. Tak.*, **8** (2019), pp. 11–38.
33) Ofosu, J. A., Masui, H. and Cho, M.: Development of a Thermal Vacuum Testing System Using Peltier Element, 65th JSASS conference (2021) pp. 1–5.